An Objectivity Algorithm for Strain Softening Material Models

Mauricio V. Donadon and Lorenzo Iannucci
Department of Aeronautics
Imperial College London
South Kensington, London SW7 2AZ, UK

Abstract

Predictive techniques for the analysis and design of metallic or composite components and structures subject to severe loading can lead to significant mesh sensitivity if cracking or tearing or penetration occurs. This is especially important for composite materials in which the material has an elastic brittle response with little or no plastic behaviour, in which energy could be dissipated. Hence, the full potential use of composite in the design of advanced composites and structures has not yet been exploited fully.

This work constitutes an effort directed towards the development of an objectivity algorithm for strain softening material models based on the 'smeared cracking formulation'. The algorithm has been implemented into LS-DYNA for hexahedron solid elements and correctly accounts for crack directionality effects. Thus enabling the control of energy dissipation associated with each failure mode regardless of mesh refinement and element topology.

The advantage of the present technique is that mesh size sensitivity on failure is removed leading to results, which converge to a unique solution, as the mesh is refined. If such a scheme were not introduced results could change significantly from mesh to mesh leading to an incorrect structural response. The proposed algorithm has been validated by a series of benchmark tests using different degrees of mesh refinement and element topologies.

1. Introduction

Numerical studies on strain localization show that in rate-independent strain softening material models the results are essentially dependent on the finite element discretization [1], [2], [3]. From the mathematical viewpoint, if softening is represented simply by a falling stress-strain curve in a rate-independent continuous material, then the partial differential equations of motion or equilibrium will change characteristic type at the onset of softening, from hyperbolic to elliptic in dynamic problems and the reverse in statics. In either case, the problem will become ill-posed, as the boundary and initial conditions for one class of equations are not appropriated for the other. As a result, it is impossible for rate-independent softening to proceed within any non-zero volume of the domain of solution. The only way is to introduce *localization* of all softening onto a surface. Displacements will be discontinuous across this surface, and in the surrounding continuous regions, there may be *unloading*, that is, decreasing stress with decreasing strain but no softening. Different methods have been presented in the open literature to correct this deficiency. One of them is the inclusion of rate-dependence in the constitutive model [4]. This may be either physical or numerical. Such an approach introduces higher temporal derivatives into the equations of motion, thereby resolving some of the issues of ill-conditioning in the face of softening. One other possibility is to make stresses in the constitutive model dependent on strain gradients [5]. This approach introduces higher special gradients into the equations of motion, again resolving some of the ill- conditioning issues. This is very difficult to program in the finite element method, since strain gradients are not normally

computed or stored. Inclusion of non-local material behaviour is also an alternative to resolve the problem. This approach makes the stresses at a point dependent on strains in a non-vanishing region around the point [6]. Mathematically this is similar to gradient-dependence, as one could regard the strains in the region around the point as Taylor series whose coefficients include higher gradients of strain at the central point. This is also very difficult to program, because the constitutive model subroutines must query surrounding elements. Ensuring proper internal dissipation during failure using a smeared cracking formulation [7, 8] is another option to avoid pathological problem associated with strain localization and mesh dependence in strain softening models. Fracture mechanics testing can quantify the *energy release rate* which is the energy required to produce a unit area of crack surface. During complete softening to zero stress, the constitutive model will dissipate energy per unit volume equal to the area beneath the stress-strain curve. To relate the two, one assumes that softening localizes into a region one element wide. Then the constitutive failure energy multiplied by the projected area of the putative crack through the element in question. This implies that the softening portion of a stress-strain curve must be adjusted according to the element size, become shallower as element become smaller. Essential energetic relationships are always preserved by using this approach. A change in the mesh topology in anticipation of material failure is another method which can be employed to resolve the problem [9]. This option clearly extends beyond the bounds of material modeling. But it is a possible direct approach to treating localization and failure. One could track conditions at the interfaces between elements rather than within elements. If conditions for the onset of softening are met, then the adjoining elements could be split apart along that boundary. At the same time, some mechanism must be introduced to dissipate the proper amount of energy in softening as stresses drop to zero. This might take the form of a simplified, temporary bridge element between the separating surfaces.

In this paper an objectivity algorithm for strain softening material models based on smeared cracking formulation is proposed to correct the mesh sensitivity problems due to strain localization in strain softening material models. The algorithm has been implemented into LS-DYNA within hexahedron solid elements and it accounts for crack directionality effects enabling the control of energy dissipation associated with different failure modes regardless of mesh refinement and element topology. The formulation is presented in a generalized context so that it can be trivially applicable to shell elements without loss of generality. The accuracy and robustness of the proposed approach is evaluated by simulating a typical in-plane tension test using finite element models with different degrees of mesh refinement and element topologies.

2. Smeared cracking approach

The idea behind the smeared cracking formulation is to relate the specific or volumetric energy, which is defined by the area underneath the stress-strain curve, with the fracture energy of the material [7, 8]. The method assumes a strain softening constitutive law for modeling the gradual stiffness reduction due to the micro-cracking process within the cohesive or process zone of the material. In order to illustrate the method, let us assume a linear-elastic-damageable material model represented by the bi-linear constitutive law shown in Fig. 1 (a).

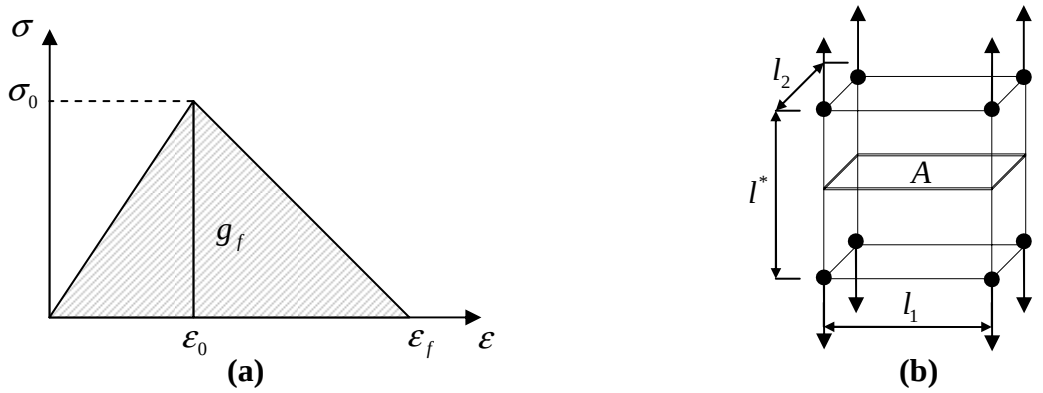

Fig.1 – Illustration of the smeared cracking concept: (a) Bi-linear constitutive law, (b) Finite element loaded in tension

For a single finite element (See Fig.1 (b)) under uniaxial deformation process, the specific energy (or energy dissipated per unit volume) is defined by the area underneath the stress-strain curve which is given by

$$g_f = \int_0^{\varepsilon_f} \sigma d\varepsilon = \frac{1}{2}\sigma_0 \varepsilon_f \tag{1}$$

The fracture energy (or energy dissipated per unit area) within a fully failed element can be written in terms of the specific energy by multiplying the specific energy by a geometric quantity defined as *characteristic length (l^*)* [8], which has a direction aligned with the loading direction and it is equal to the height of the element (See Fig.1 (b)) that is,

$$G_f = g_f l^* = \frac{1}{2}\sigma_0 \varepsilon_f l^* \tag{2}$$

The dimension of the elements which defines the *characteristic length* must satisfy the following condition in order to ensure material stability,

$$l^* \geq \frac{G_f}{g_f} \tag{3}$$

and the softening modulus H is defined as a function of the characteristic length and the material fracture energy as follows,

$$H = \frac{\sigma_0^2 l^*}{\sigma_0 l^* \varepsilon_0 - 2G_f} \tag{4}$$

The correction of the softening slope H according to the finite element size, as proposed by Bazant [8], seems an attractive solution to avoid mesh dependence however, the approach has some limitations. Firstly, the crack growth direction must be parallel to one edge of the finite element, which is not the case for multi-directional composite laminates for instance, where layers can have arbitrary directions. Secondly, it cannot handle non-structured meshes required in most of the complex finite element models with geometric discontinuities. In order to

overcome such limitations and to ensure the objectivity of the model for generalized situations, a methodology originally proposed by Oliver [10] for shell elements has been used and extended to handle solid elements subjected to multidirectional failure. The dependence of the characteristic length on the fracture energy as well as its mathematical expression, were derived based in the work proposed by Oliver [10]. The method ensures a constant energy dissipation regardless of mesh refinement, crack growth direction and element topology so that, it is still applicable to non-structured meshes.

3. Objectivity algorithm

3.1 Energy dissipated within a curvilinear singular band

Consider a planar singular band in a hypothetical solid shown in Fig. 2

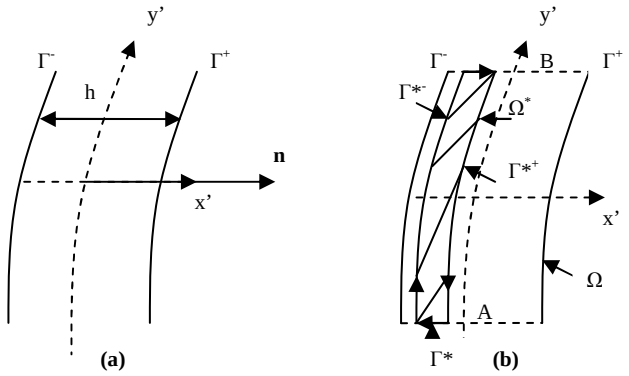

Fig.2 – Analysis within a singular band [10]

Using Taylor's series Oliver [10] showed that the displacement vector u between two boundary lines Γ^- and Γ^+ of a planar singular band can be expanded from its value in the boundary line and it is given in curvilinear coordinates as follows,

$$u(x^{'}, y^{'}) \cong u^{-}(y^{'}) + \vartheta(x^{'}, y^{'})\Delta u(y^{'}) \tag{5}$$

where $\Delta u(y^{'}) = u^{+}(y^{'}) - u^{-}(y^{'})$ is defined as a relative displacement between the two boundary lines Γ^- and Γ^+ and $\vartheta(x^{'}, y^{'})$ is a function to be determined. By inspecting Eq. (5) it can be clearly seen that,

$$\vartheta(x^{'}, y^{'}) = \begin{cases} 0 & in \quad \Gamma^{-} \\ 1 & in \quad \Gamma^{+} \end{cases} \tag{6}$$

Now enforcing equilibrium across the singular band and applying the Gauss's theorem, one can show that the energy dissipated within the band is given by,

$$W^{*} = G_f \int_{\Omega^*} \frac{\partial \vartheta}{\partial x^{'}} d\Omega^{*} = \int_{\Omega^*} g_f \, d\Omega^{*} \tag{7}$$

which leads to the following relationship between fracture energy and specific energy,

$$g_f = G_f \frac{\partial \vartheta}{\partial x'} = \frac{G_f}{l^*} \tag{8}$$

Where the characteristic length is written in terms of the partial derivatives of $\vartheta(x', y')$ as follows,

$$l^*(x', y') = \left(\frac{\partial \vartheta}{\partial x'} \right)^{-1} \tag{9}$$

3.2 Determination of the characteristic lengths

In order to apply the theory presented in the previous section to the discretized medium, consider a mesh of C^0 continuous hexahedron orthotropic solid elements (See Fig. 3).

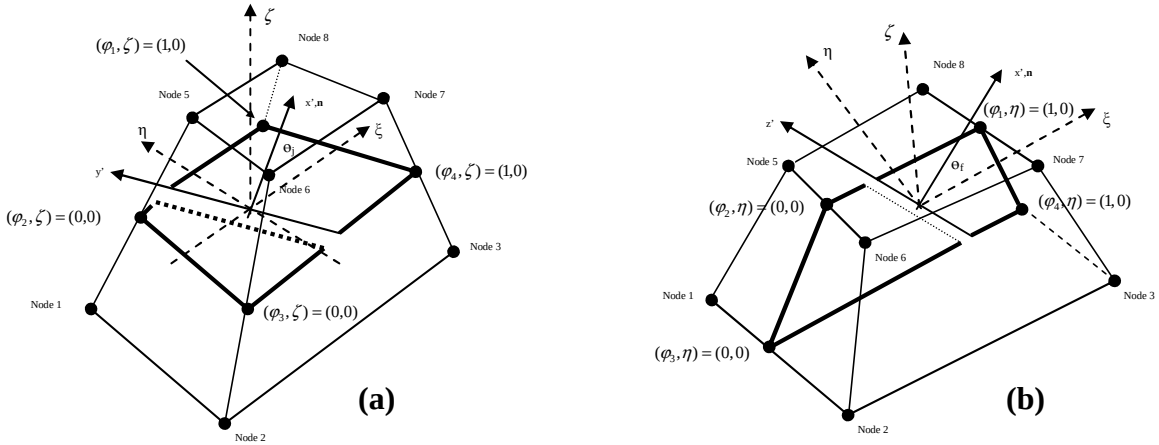

Fig. 3 – Determination of the characteristic lengths: (a) Virtual plane for in-plane failure modes; (b): Virtual plane for out-of-plane failure modes

A set of cracked elements is determined by using appropriated failure criteria for detecting the crack initiation. For composite laminates for instance, the crack orientation depends on the fiber orientation. The cracked plane is defined here as a normal vector which is parallel to the fibers for fiber failure and normal to the fiber direction for matrix failure. From equation (7) the function ϑ has to be continuous and derivable, satisfying Eq. (5) . A simple function defined in the isoparametric coordinates ξ and η which fulfils these requirements for the in-plane failure modes is

$$\vartheta(\xi, \eta) = \sum_{i=1}^{n_c} N_i(\xi, \eta) \vartheta_i \tag{10}$$

Where n_c is the number of corner nodes of a virtual plane located at the midplane of the element ($n_c = 4$ for our case), N_i are the standard C^0 shape functions of an element of n_c virtual nodes in its midplane and ϑ_i is the value of the ϑ at corner i. If the crack location inside the element is known, ϑ_i takes the value +1 if the corner node i is ahead, and 0 otherwise. The function defined by Eq. (10) fulfils the required condition of continuity within the elements and takes the

values +1 for the nodes on the boundaries ahead the crack and 0 for the nodes on the boundaries behind the crack. In general, however, the exact location is not known and usually only some indication of the onset of cracking and the crack directions is obtained at the integration points. Following the methodology proposed by Oliver (1989) one can assume an auxiliary coordinate system at each integration point j as shown in Figs. 3 (a) and 3 (b). The direction of the local axis $x^{'}$ is defined by the normal to the fracture plane, which is the fiber angle ($\theta_j = \theta_{fibre}$) or the local warp direction for fabrics ($\theta_j = \theta_{warp}$) and ($\theta_j = \theta_{fibre} + 90^0$) for matrix failure or ($\theta_j = \theta_{warp} + 90^0$) for failure in the weft direction when fabrics are considered. This leads to the following coordinate's transformation,

$$\begin{Bmatrix} x_i^{'} \\ y_i^{'} \end{Bmatrix} = \begin{bmatrix} \cos(\theta_j) & \sin(\theta_j) \\ -\sin(\theta_j) & \cos(\theta_j) \end{bmatrix} \begin{Bmatrix} x_i \\ y_i \end{Bmatrix} \tag{11}$$

Where the values of ϑ at each corner are established according to their position with respect to the local axis $(x^{'}, y^{'})$, ($\vartheta_i = 1$ if $x_i^{'} \geq 0$, otherwise $\vartheta_i = 0$). The characteristic length associated with fiber failure or failure in the warp direction either in tension or compression, at the present integration point j with isoparametric coordinates ξ_j and η_j and cracking angle θ_j is obtained as

$$l_{11}^t = l_{11}^c = \left(\frac{\partial \vartheta(\xi_j, \eta_j)}{\partial x^{'}} \right)^{-1} = \left(\sum_{i=1}^{n_c} \left[\frac{\partial N_i(\xi_j, \eta_j)}{\partial x} \cos(\theta_{fibre}) + \frac{\partial N_i(\xi_j, \eta_j)}{\partial y} \sin(\theta_{fibre}) \right] \vartheta_i \right)^{-1} \tag{12}$$

and the characteristic length associated with matrix tensile failure or failure in the weft direction is given by

$$l_{22}^t = \left(\sum_{i=1}^{n_c} \left[-\frac{\partial N_i(\xi_j, \eta_j)}{\partial x} \sin(\theta_{fibre}) + \frac{\partial N_i(\xi_j, \eta_j)}{\partial y} \cos(\theta_{fibre}) \right] \vartheta_i \right)^{-1} \tag{13}$$

where

$$\begin{Bmatrix} \frac{\partial N}{\partial x} \\ \frac{\partial N}{\partial y} \end{Bmatrix} = J_{xy}^{-1} \begin{Bmatrix} \frac{\partial N}{\partial \xi} \\ \frac{\partial N}{\partial \eta} \end{Bmatrix} \tag{14}$$

And J_{xy} is defined as the in-plane Jacobian matrix given by

$$J_{xy} = \begin{bmatrix} \frac{\partial x}{\partial \xi} & \frac{\partial y}{\partial \xi} \\ \frac{\partial x}{\partial \eta} & \frac{\partial y}{\partial \eta} \end{bmatrix} \tag{15}$$

Where the partial derivatives with respect to the isoparametric coordinates are written as

$$\frac{\partial x}{\partial \xi} = \frac{1}{4}(1+\xi)x_1 - \frac{1}{4}(1+\xi)x_2 - \frac{1}{4}(1-\xi)x_3 + \frac{1}{4}(1-\xi)x_4 \tag{16}$$

$$\frac{\partial x}{\partial \eta} = \frac{1}{4}(1+\eta)x_1 + \frac{1}{4}(1-\eta)x_2 - \frac{1}{4}(1-\eta)x_3 - \frac{1}{4}(1+\eta)x_4 \tag{17}$$

$$\frac{\partial y}{\partial \xi} = \frac{1}{4}(1+\xi)y_1 - \frac{1}{4}(1+\xi)y_2 - \frac{1}{4}(1-\xi)y_3 + \frac{1}{4}(1-\xi)y_4 \tag{18}$$

$$\frac{\partial y}{\partial \eta} = \frac{1}{4}(1+\eta)y_1 + \frac{1}{4}(1-\eta)y_2 - \frac{1}{4}(1-\eta)y_3 - \frac{1}{4}(1+\eta)y_4 \tag{19}$$

Where the pairs (x_i, y_i) refers to the global coordinates of the virtual nodes defining the midplane of the element (See Fig. 3(a)). In-plane shear cracking is strongly dependent on the fiber orientation within the element therefore, the characteristic length associated with in-plane shear failure has been assumed to be the same as the one defined for fiber failure or failure in the warp direction, that is, $l_{12}^s = l_{11}^t = l_{11}^c$.

For the out-of-plane failure modes such as transverse compression failure and out-of-plane shear failure, a second virtual plane perpendicular to the one defined previously has been defined (Fig. 3 (b)).Without loss of generality the function ϑ can be rewritten as,

$$\vartheta(\xi, \zeta) = \sum_{i=1}^{n_c} N_i(\xi, \zeta)\vartheta_i \tag{20}$$

Where n_c is the number of corner nodes of a transverse virtual plane located at the midplane of the element according to Fig. 3(b). N_i are the linear shape functions defined previously and n_c is the number of virtual nodes defining the cracking plane and ϑ_i is the value of the ϑ function at corner i. x', z' is an auxiliary coordinate system defined at the centre of the element, this being identified by the values of the isoparametric coordinates ($(\xi = 0, \eta = 0, \zeta = 0)$ with the direction of the local axis x' defined by the normal to the fracture plane,

$$\begin{Bmatrix} x_i' \\ z_i' \end{Bmatrix} = \begin{bmatrix} \cos(\theta_j) & \sin(\theta_j) \\ -\sin(\theta_j) & \cos(\theta_j) \end{bmatrix} \begin{Bmatrix} x_i \\ z_i \end{Bmatrix} \tag{21}$$

The values of ϑ at each corner node are established according to their position with respect to the local axis (x', z'), ($\vartheta_i = 1$ if $x_i' \geq 0$, otherwise $\vartheta_i = 0$) in a similar way as the one described previously. The characteristic length associated with transverse compression failure or compression failure in the weft direction is given as a function of the fracture angle as follows,

$$l_{22}^c = \left(\frac{\partial \vartheta(\xi_j, \zeta_j)}{\partial x'} \right)^{-1} = \left(\sum_{i=1}^{n_c} \left[\frac{\partial N_i(\xi_j, \zeta_j)}{\partial x} \cos(\theta_f) + \frac{\partial N_i(\xi_j, \zeta_j)}{\partial z} \sin(\theta_f) \right] \vartheta_i \right)^{-1} \tag{22}$$

where

$$\begin{Bmatrix} \dfrac{\partial N}{\partial x} \\ \dfrac{\partial N}{\partial z} \end{Bmatrix} = J_{xz}^{-1} \begin{Bmatrix} \dfrac{\partial N}{\partial \xi} \\ \dfrac{\partial N}{\partial \zeta} \end{Bmatrix} \tag{23}$$

And J_{xy} is defined as the out-of-plane Jacobian matrix given by

$$J_{xz} = \begin{bmatrix} \dfrac{\partial x}{\partial \xi} & \dfrac{\partial z}{\partial \xi} \\ \dfrac{\partial x}{\partial \zeta} & \dfrac{\partial z}{\partial \zeta} \end{bmatrix} \tag{24}$$

Where the partial derivatives with respect to the isoparametric coordinates are written as

$$\frac{\partial x}{\partial \xi} = \frac{1}{4}(1+\xi)x_1 - \frac{1}{4}(1+\xi)x_2 - \frac{1}{4}(1-\xi)x_3 + \frac{1}{4}(1-\xi)x_4 \tag{25}$$

$$\frac{\partial x}{\partial \zeta} = \frac{1}{4}(1+\zeta)x_1 + \frac{1}{4}(1-\zeta)x_2 - \frac{1}{4}(1-\zeta)x_3 - \frac{1}{4}(1+\zeta)x_4 \tag{26}$$

$$\frac{\partial z}{\partial \xi} = \frac{1}{4}(1+\xi)z_1 - \frac{1}{4}(1+\xi)z_2 - \frac{1}{4}(1-\xi)z_3 + \frac{1}{4}(1-\xi)z_4 \tag{27}$$

$$\frac{\partial z}{\partial \zeta} = \frac{1}{4}(1+\zeta)z_1 + \frac{1}{4}(1-\zeta)z_2 - \frac{1}{4}(1-\zeta)z_3 - \frac{1}{4}(1+\zeta)z_4 \tag{28}$$

Where the pairs (x_i, z_i) refers to the global coordinates of the virtual nodes defining the midplane of the element. For out-of-plane shear failure modes, cracks are assumed to be smeared over the thickness of the element with crack a crack band defined between upper and lower faces of the element which is equivalent to assume $\theta_f = 90^0$ in Eq. (22) ,

$$l_{13}^s = l_{23}^s = \left(\sum_{i=1}^{n_c} \left[\frac{\partial N_i(\xi_j, \zeta_j)}{\partial z} \right] \vartheta_i \right)^{-1} \tag{29}$$

4. Mesh sensitivity study

In order to evaluate the performance of the algorithm, a simple coupon test simulation assuming the linear-elastic-damageable material model shown in Fig. 1(a) has been carried out. The dimensions of the composite virtual coupon consisted of 20x10x2mm^2 which represents a small volume of the material under uniaxial stress. The virtual coupon was discretized using six different mesh densities three of them being non-structured meshes according to Fig. 4. The

composite specimen was continuously loaded in the fiber direction under displacement control to mimic a pseudo-static loading on the virtual coupon with mechanical properties given in Table 1.

Table 1 – Typical mechanical properties for orthotropic layers	
E_x	100.00 GPa
$E_y=E_z$	8.11 GPa
ν_{xy}	0.3 GPa
$G_{xy}= G_{xz}= G_{yz}$	4.65 GPa
σ_0	2000.00 MPa
G_f	50 kJ/m^2

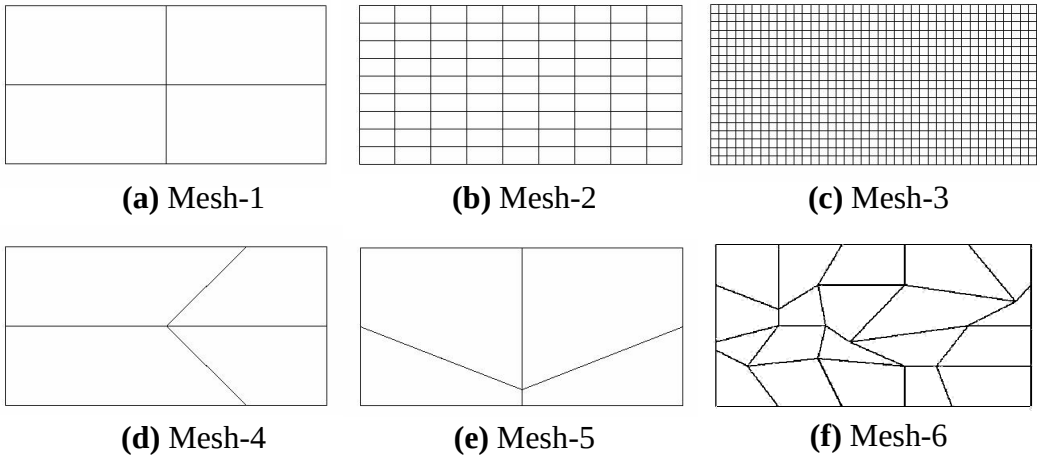

Fig. 4 – Meshes used in the mesh sensitivity study

For comparison purposes, the load-displacement responses for all meshes were compiled in a single graph where the dissipated energy is defined by the area underneath the force-displacement curves. Fig. 5 compares the structural response obtained using the different mesh types.

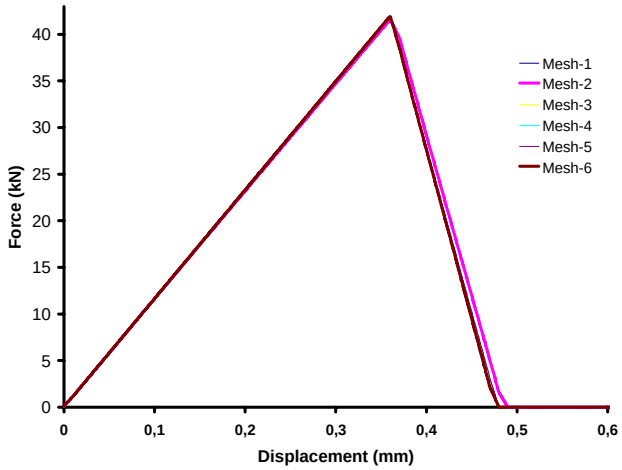

Fig. 5 – Effect of mesh refinement on the structural response

According to Fig. 5 the energy dissipated in the formation of crack is clearly mesh insensitive. The structural responses are almost identical ensuring the control of the energy dissipation regardless of mesh refinement and element topology. Minor differences may be attributed to rounding errors within the FE code. For explicit dynamic FE codes the failure location is defined by both rounding errors in the uniform stress field associated with the viscosity terms used within the FE code to smear the wave over a series of elements, and the corresponding wave reflections within the FE mesh. These two effects acting simultaneously define a band of failed elements which in practice intends to mimic the fracture in the real structural component. Fig. 6 depicts the failure locations for the meshes studies in this section.

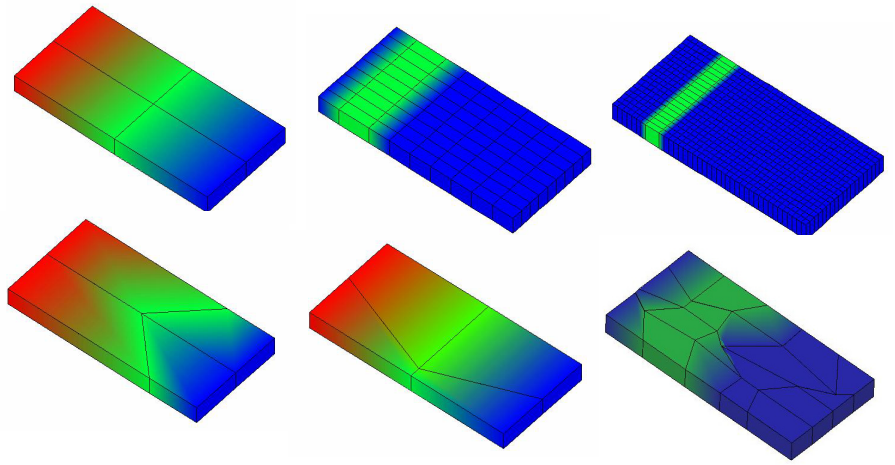

Fig. 6 – Failure localization for different mesh types

5. Conclusions

This paper presents a detailed formulation and numerical implementation of an objectivity algorithm for strain softening material models. The approach has shown to be robust resolving the mesh dependence problems existing in strain softening models, enabling failure prediction within an energy based framework. The robustness of the algorithm is illustrated by simulating a unidirectional orthotropic laminate loaded in tension using models with different mesh densities and element topologies. The numerical results indicated that the energy dissipated to create the crack is independent on the mesh used. The formulation is presented in a generalized way so that it can be easily modified to handle different element types covering a full range of finite elements including beams, shell and solids.

6. Acknowledgements

The authors acknowledge the financial support received for this work from the Brazilian National Research Council (CNPq), process 200863/00-2 (NV)

References

[1] Sluys L. J., De Borst R., "Wave propagation and localization in rate-dependent cracked medium – Model formulation and one-dimensional examples", *Int. J. Solids & Structures*, Vol. 29, pp. 2945-2958, 1992.

[2] Sluys L. J., De Borst R., "Wave propagation and dispersion in a gradient-dependent medium", *Int. J. Solids & Structures*, Vol. 30, pp. 1153-1171, 1993.

[3] De Borst R., "Damage, material instabilities and failure", *Encyclopedia of Computational Mechanics*, Wiley, Chichester, Vol. 2, Chapter 10, 2004.

[4] Needleman A., "Material rate dependence and mesh sensitivity in localization problems", *Comp. Meth. in Appl. Mech. and Engineering*, Vol. 63, pp. 69-85, 1988.

[5] Aifantis E. C., "The physics of plastic deformation", *Int. J. Plasticity*, Vol. 3, pp. 211-247, 1987.

[6] Bazant Z., "Mechanics of distributed cracking", *Appl Mech Rev*, Vol. 39, pp. 675-705, 1986.

[7] Pijaudier-Cabot G. et al, "Comparison of various models for strain softening ", *Eng. Comput.*, Vol. 5, pp. 141-150, 1988.

[8] Bazant Z., "Crack band theory for fracture of concrete", *Materiaux et Constructions*, Vol. 16 (93), 1983.

[9] Hillerborg A. et al, "Analysis of crack formation and crack growth in concrete by means of fracture mechanics and finite elements", *Cement and Concrete Research*, Vol. 6, pp. 773-782, 1976.

[10] Oliver J., "A consistent characteristic length for smeared cracking model", *Int Journal for Num. Methods in Engineering*, Vol. 28, pp. 461-474, 1989.